

# Cold Compaction Behavior of Nano and Micro Aluminum Powder under High Pressure

Dasom Kim\*, Kwangjae Park\*, Kyungju Kim\*\*, Seungchan Cho\*\*\*, Yusuke Hirayama\*\*\*\*, Kenta Takagi\*\*\*\*\*†, Hansang Kwon\*\*\*\*\*†

**ABSTRACT:** In this study, micro-sized and nano-sized pure aluminum (Al) powders were compressed by unidirectional pressure at room temperature. Although neither type of Al bulk was heated, they had a high relative density and improved mechanical properties. The microstructural analysis showed a difference in the process of densification according to particle size, and the mechanical properties were measured by the Vickers hardness test and the nano indentation test. The Vickers hardness of micro Al and nano Al fabricated in this study was five to eight times that of ordinary Al. The grain refinement effect was considered to be one of the strengthening factors, and the Hall-Petch equation was introduced to analyze the improved hardness caused by grain size reduction. In addition, the effect of particle size and dispersion of aluminum oxide in the bulk were additionally considered. Based on these results, the present study facilitates the examination of the effect of particle size on the mechanical properties of compacted bulk fabricated by the powder metallurgy method and suggests the possible way to improve the mechanical properties of nano-crystalline powders.

**Key Words:** Aluminum, Powder metallurgy, Nanocrystalline material, Hall-Petch equation, Oxide dispersion strengthening

## 1. INTRODUCTION

Recently, lightweight material has been needed in transportation equipment for automobiles, aerospace, and shipping to increase fuel efficiency. Aluminum (Al), which is a low-cost, common material, has been widely used as a light material. Although Al is light and has high elongation, it is too soft to be used as a substitute material for steel. Thus, Al has been used in the form of composites with aluminum alloys or other materials to compensate for its relatively low strength although it is light and ductile, such as the Al-Al<sub>2</sub>O<sub>3</sub> composite, Al-stainless(SUS) composite, and Al-carbon nanotubes(CNT) composite [1-3]. Attempts have been made to improve the mechanical properties by controlling grain size. Studies on nano-crystalline materials that realize excellent mechanical

properties have been carried out by many researchers. Meyers *et al.* introduced fabrication methods for nano-crystalline powder, such as mechanical milling and inert gas condensation [4]. Hirayama *et al.* fabricated a high purity nano Al powder with fine particle size control over an average particle size of 80 to 240 nm according to the pressure in the main chamber during the thermal plasma process [5].

However, nano powder is difficult to densify due to large friction, and the grain growth of crystals occurs rapidly when heated. Ye *et al.* have produced powders through cryo-milling and sintering at low pressure with spark plasma sintering (SPS) at 80 MPa to fabricate nano-crystalline Al5083, however, the mechanical properties of the nano powder did not considerably improve [6]. Fang *et al.* showed that nano-crystalline-cemented tungsten carbide was bulk-processed by hot

Received 13 March 2019, received in revised form 27 June 2019, accepted 28 June 2019

\*Department of Materials System Engineering, Pukyong National University, Busan, Korea

\*\*The International Science Technology Research Center, Pukyong National University, Busan, Korea

\*\*\*Department of Composites Research, Korea Institute of Materials Science, Changwon, Korea

\*\*\*\*Magnetic Powder Metallurgy Research Center, National Institute of Advanced Industrial Science and Technology (AIST)

\*\*\*\*\*Department of R&D, Next Generation Materials Co., Ltd., Busan, Korea,

†Corresponding authors, Dr. Takagi Kenta (E-mail: k-takagi@aist.go.jp) and Prof. Hansang Kwon (E-mail: kwon13@pknu.ac.kr)

pressing, SPS, and hot isostatic pressing. As a result, the WC-Co fabricated by SPS has fine grain size, which also show high hardness value [7]. However, as the particle size became finer, the grain size increased rapidly as the temperature increased. When powder is sintered by the SPS process, it can be densified at low temperature by increasing the pressure. Then, grain size growth is suppressed, and high pressure subjects the materials to deformation, so that strain can accumulate in the grains. Pure alumina with a grain size of 200 nm was sintered with over 400 MPa. As the pressure was increased from 200 MPa to 500 MPa, the toughness and hardness of material increased [8]. Although some researchers have tried to sinter hard material powder with high pressure, no studies about Al pressed with ultra-high pressure ( $> 1$  GPa) have been reported.

In this study, we tried to control the crystallite size in Al bulk by compaction of Al powder with ultra-high pressure at room temperature. To control the amount of alumina formed on the surface of the nano powder with a very large specific surface area, the effect of the alumina oxide amount on the mechanical properties was minimized. The mechanical and electrical properties as well as the microstructure of the micro Al and nano Al powders were investigated. XRD analysis and oxygen content analysis were performed to compare the degree of oxidation, and the enhancement mechanism was supplemented by further considering the particle size and dispersion of the oxides.

## 2. EXPERIMENTAL PROCEDURE

### 2.1 Characterization of raw powder

The micro-sized Al powder (ECKA Granules, Japan Co. Ltd., purity 99.85%, particle size 100  $\mu\text{m}$ ), which was fabricated by gas atomization, and the nano-sized Al powder, which was fabricated by a thermal plasma process with 45  $\mu\text{m}$  pure Al (purity 99.99%, Kojundo Chemical Lab. Co., Ltd., Japan), were prepared in a glove box with the oxygen level maintained below 1 ppm (JEOL Co., Ltd.). Each Al powder was analyzed by XRD (Rigaku, Ultima IV, Japan) with a Cu K $\alpha$  radiation source ( $\lambda = 1.5148$  Å, 40 kV, and 40 mA). The range of  $2\theta$  obtained using a linear detector (D/tex ultra) was 20°–80°, the step size was 0.02°, and the scan rate was 0.06°/s. The powders were also observed through SEM with EDS (TESCAN, VEGA II LSU, Czech). The laser diffraction particle size analyzer (PSA) was used to measure the mean particle size of the micro powder (BECKMAN COULTER (USA), LS 13320). In the case of nano powder, the particle size distribution was measured with SEM images. The oxygen content was analyzed with an elemental analyzer (Elementar Anlaysiaensysteme GmbH, Germany).

### 2.2 Fabrication of Al bulk

A tungsten cobalt mold ( $\phi 6$  mm) containing Al powder was installed in the chamber of a spark plasma sintering machine

(Fuji Electronic Industrial Co., Ltd., SPS-321Lx, Japan). In the case of nano Al powder, the powder was poured into a mold soaked with heptane in a glove box. Then, micro and nano Al powders were compacted with 1.2 GPa pressure at room temperature (about 20°C) for 1 min in a vacuum.

### 2.3 Characterization of bulk

The density of the compacted Al samples was measured using the Archimedes method with a densitometer (KERN ABJ, 120-4M). To analyze the mechanical properties, a Vickers hardness test (HM-101, Mitutoyo Corporation, Japan) according to JIS B 7725, ISO 6507-2 standards was conducted with a load of 0.3 kg. The microstructure of the cross section of each sample was observed with SEM and EDS (TESCAN, VEGA II LSU, Czech). Elemental mapping was conducted to determine the constituent elements of the material (HITACHI, S-2400, Japan). Finally, to confirm the relationship between the grain size and tensile strength, we used the Hall-Petch equation, in which the grain size was substituted with the crystallite size, calculated using the Scherrer equation with XRD (Rigaku, Ultima IV, Japan) data analysis with a Cu K $\alpha$  radiation source ( $\lambda = 1.5148$  Å, 40 kV, and 40 mA). The range of  $2\theta$  obtained using a linear detector (D/tex Ultra, Tokyo, Japan) was 20°–80°, the step size was 0.02°, and the scan rate was 0.06°/s.

The electrical conductivity of samples was measured with an eddy current conductivity tester (TMD-102, TM Teck) at room temperature. The oxygen content of the Al powder was measured under the same conditions.

## 3. RESULTS AND DISCUSSION

Fig. 1 shows the SEM micrographs of each powder. Fig. 1(a) shows that the nano Al powder has a spherical shape, and the powder tends to aggregate. Conversely, the micro-sized powder has an elongated shape, its surface is relatively rough, and the particles do not cohere with each other as shown in Fig. 1(b).

Fig. 2 shows the PSA graph of micro Al and nano Al powders. Micro Al has an average particle size of 145  $\mu\text{m}$ , which is 1800 times the nano Al particle size of 79 nm. Micro Al has a maximum volume content of less than 9% by particle diameter, and nano Al has a maximum volume content of 31% by

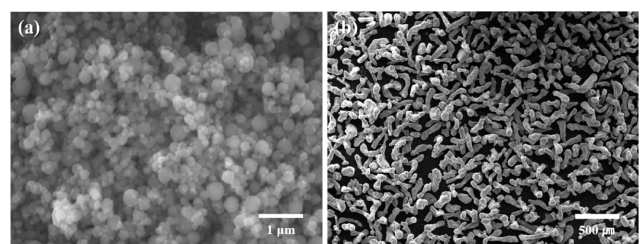


**Fig. 1.** SEM micrographs of (a) nano pure Al powder and (b) micro pure Al powder

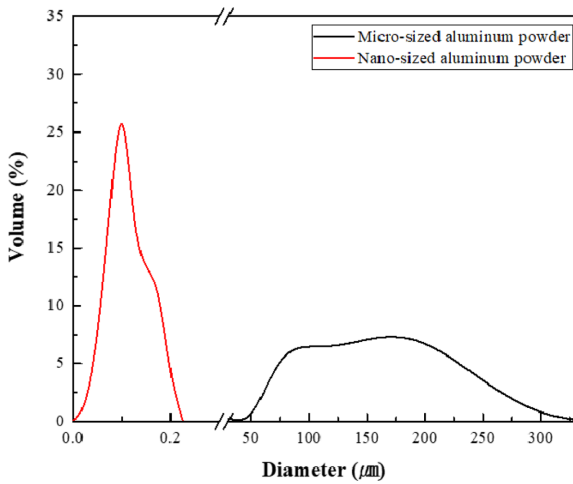


Fig. 2. PSA graph of nano- and micro-sized pure Al powders

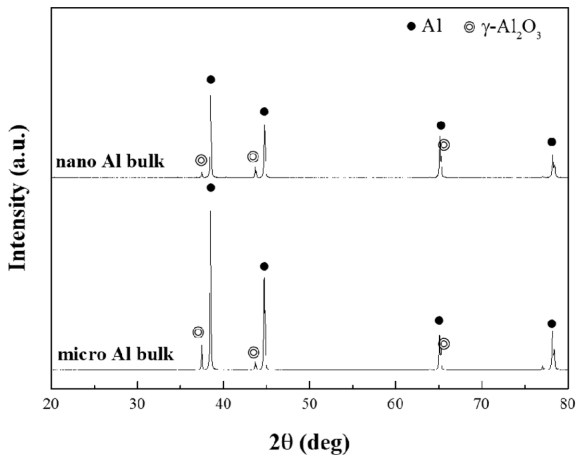


Fig. 3. XRD graphs of pure aluminum materials compacted nano and micro powders

particle diameter, which means that the dispersion degree of nano Al is higher than that of micro Al powder. In addition, the difference between the maximum particle size and the minimum particle size of micro and nano Al powders was approximately 80% and 85%, respectively. Therefore, although the two powders differed in their degree of dispersion and distribution, they were considered suitable for a comparison of nano-sized and micro-sized powders.

Fig. 3 shows the XRD results for each compacted body. Each powder was bulked by unidirectional compression with a pressure of 1.2 GPa at room temperature. The phases on the surface of the bulk formed from each powder were observed with XRD analysis. Al and Al oxide phase ( $\text{Al}_2\text{O}_3$ ) were detected in each sample, and no other phase was detected. It was confirmed to be pure Al. The following are SEM micrographs and EDS results of cross sections of each sample, which are shown in Figs. 4 and 5.

Fig. 4 shows the FE-SEM microstructures and EDS results of the cross section of the compacted bulk from nano powder.

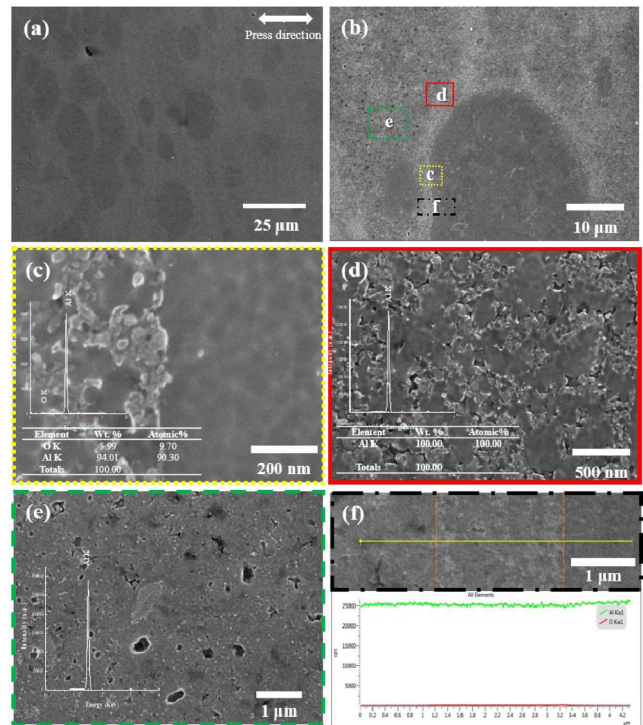
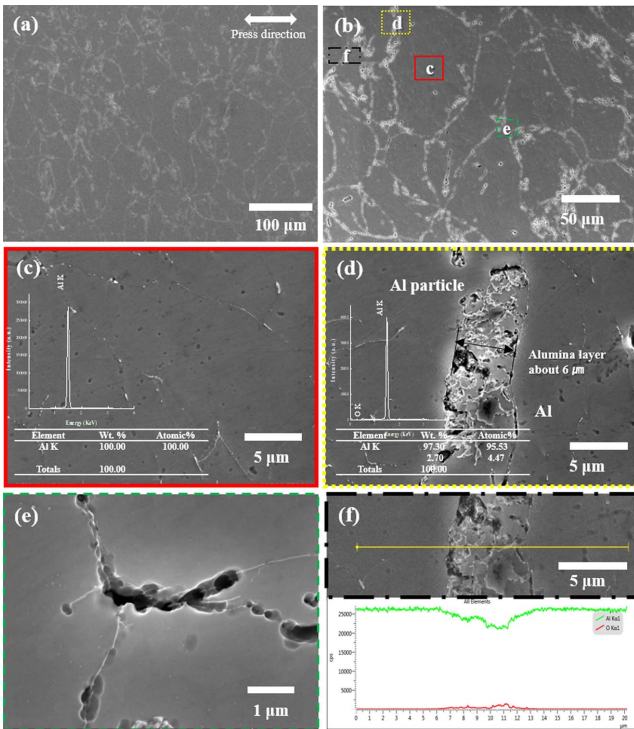


Fig. 4. FE-SEM micrographs of (a) pure Al compacted body with nano-sized powder, (b) high magnification of (a); (c) SEM micrograph and EDS of left-side structure in part 1 of (b); (d) SEM and EDS in part 2 of (b); and (e) part 3 of (b); (f) line mapping result though all regions marked in (b)

First, SEM images of low magnification were divided into three regions, and each region as observed. In this case, as shown in (a), it can be observed that micro-sized particles are distributed. In Fig. 4(c), the microstructures observed at high magnification show that large particles and the interfaces between the large particles and matrix showed almost no pores. The large particles are densified with almost no pores. As can be seen in Fig. 4(e), high magnification of the portion directly surrounding the large particle shows that little trace of the spherical particles can be observed, and some of large pores remaining after the particles were bulked is observed. On the other hand, the more distant part, Fig. 4(d), shows that the spherical powder is better preserved than in Fig. 4(e), and finer pores remain. Two factors were considered for this difference in each area. First, it seems that this difference occurred because there was already a mass of agglomerated powder. The agglomerated mass behaves like a large particle, and when pressed under the same pressure, it is more easily compressed and densified, and appears as a large agglomerated particle, as shown in (a). The second is the influence of the alumina layer. If coarse particles are generated in some places due to the phenomenon of powder clustering as described above, there will also be a difference in the amount of alumina generated per unit volume. Where only nano pow-





**Fig. 5.** FE-SEM micrographs of (a) pure aluminum compacted body with micro-sized powder, (b) high magnification of (a); (c) SEM micrograph and EDS of aluminum powder region of part 1 in (b); (d) SEM and EDS of grain boundary in part 2 of (b); and (e) EDS in part 3 of (b); (f) result of line mapping through all regions marked in (b)

ders are present, an alumina layer surrounds the particle surface, so when pressure is applied, more force is required to deform it due to its brittle surface. However, as shown in Fig. 4(f), when line profile analysis was performed across each region, it can be observed that the difference in oxygen content is almost constant, and the influence is not significant.

Fig. 5 shows the FE-SEM microstructures of the cross section of the compacted bulk with micro-sized aluminum powder. It is clear that the pore size and particle interface are evident when compared with nano powder. First, Fig. 5(d) shows the interface between the particles, and the particle at high magnification. The interface, which has a thickness of approximately 6  $\mu\text{m}$ , is an oxidized layer resulting from the line profile. The interface has a relatively high oxygen content (Fig. 5(f)). As confirmed by the XRD results, it was thought that an alumina layer existed on the powder surface. Fig. 5(e) shows the pores of this material, and the pores are generated at the contact point of three particles where stress is concentrated. The pores along the grain boundary are bigger than that of nano Al and elongated. The results of line profile between the particles shown in Fig. 4(f), the interface was oxidized more than that of nano size Al.

Compaction can be divided into the four stages shown in Fig. 6. In the first step, independent particles are filled. When

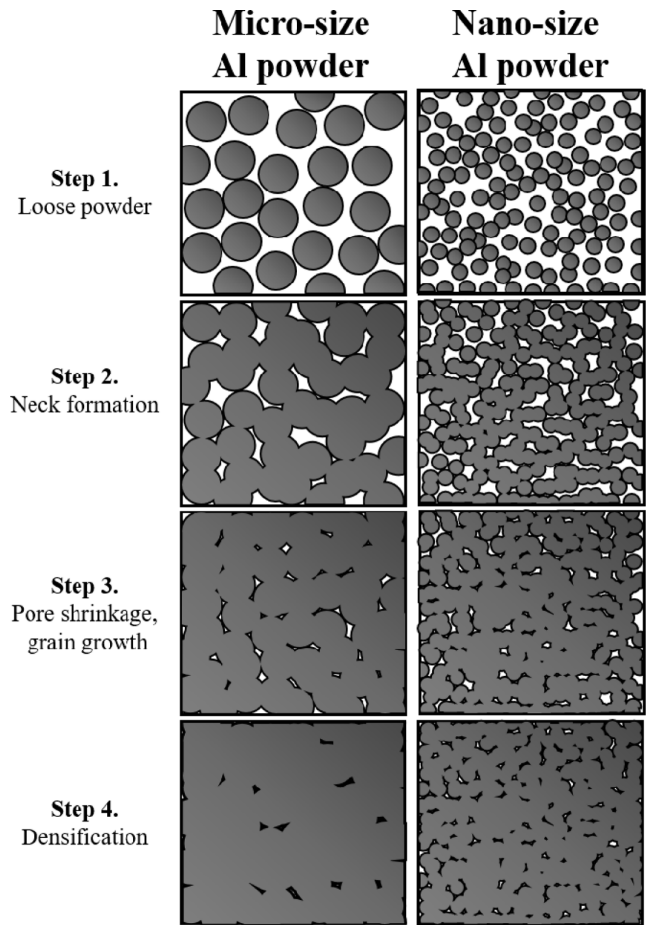


**Fig. 6.** Illustration of sintering stage of general spark plasma sintering process of micro- and nano-sized powders

compressive pressure is applied, a neck is formed as the coordination number increases. As the size of the neck gradually increases, the pores existing between the particles shrink and densification begins. The rate of growth of the neck and the degree of final densification are affected by the temperature and pressure during processing. In this study, we tried to densify only with pressure. In the case of aluminum, when 200 MPa pressure is applied to general micro-sized particles, the densification is nearly 100%. However, as the particle size becomes smaller, the initial packing density is reduced, and the dislocation density that can accumulate in one powder decreases. Thus, processing becomes difficult. Therefore, it is very difficult to densify nanoparticles to 100%, and high pressure is required to achieve this. As a result, at the completion of the bulking process, one article is deformed more in the case of micro Al, and the pores remain relatively large and less, but in the case of the nano powder, the shape of the spherical powder is mostly maintained, and many smaller pores remain.

Fig. 7 shows the Vickers hardness values for nano Al and micro Al, which are 52.94 HV and 79.60 HV, respectively. In order to analyze the mechanical properties more precisely,

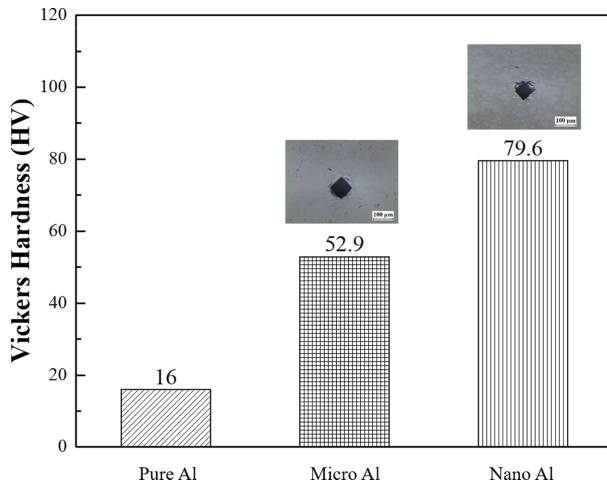


Fig. 7. Graph of Vickers hardness for compacted body of micro Al and nano Al [9]

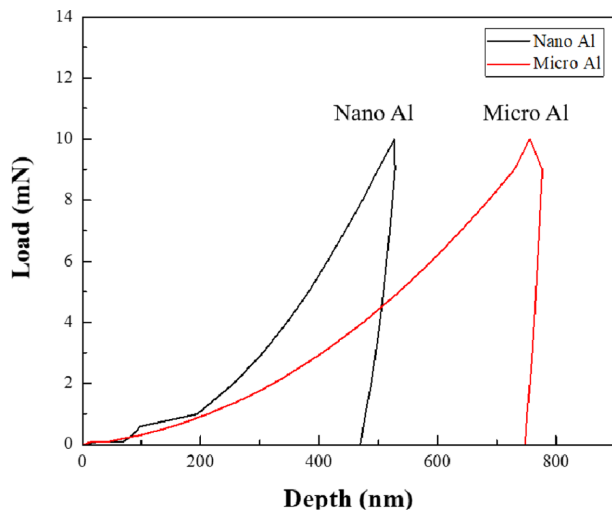


Fig. 8. Nanoindentation (load-depth) graph of micro Al and nano Al

nanoindentation was performed on micro Al and nano Al (Fig. 8). The Vickers hardness values for nanoindentation of micro Al and nano Al were 62.18 HV and 150.99 HV, respectively. In addition, when the same force was applied, the indenter insertion depth was found to be deeper for nano Al than for micro Al, indicating that nano Al showed higher mechanical strength even though the densification was relatively lower. Srivatsan *et al.* studied the variation in the particle size of tungsten carbide powders. It was confirmed that when the powder size increased six-fold, the hardness value increased 1.5-fold [10]. Thus, the size and mechanical properties of a particle are related. This correlation was predicted to be a result of grain size reduction and can be explained by the Hall-Petch equation [11].

The  $\sigma_H$  is the Vickers hardness of the material, and  $\sigma_0$  is the material constant.  $K_y$  is the strengthening coefficient, and  $d$

denotes the grain size of the material. Indeed, many researchers have argued that the reinforcement of the material is due to grain refinement and have explained this by citing the Hall-Petch equation [12-14]. Jang *et al.* measured crystallite size by applying the XRD results to the Scherrer equation and substituting it into the Hall-Petch equation to calculate the hardness value [15]. In this study, the crystallite size obtained by XRD of nano Al was 43.23 nm, calculated by substituting the material constant for 99.99% Al ( $\sigma_0 = 11.3$  MPa,  $K_y = 0.07$  MPa  $m^{0.5}$  by Farhat *et al.* The result was 35.43 HV (347.97 MPa) [16].

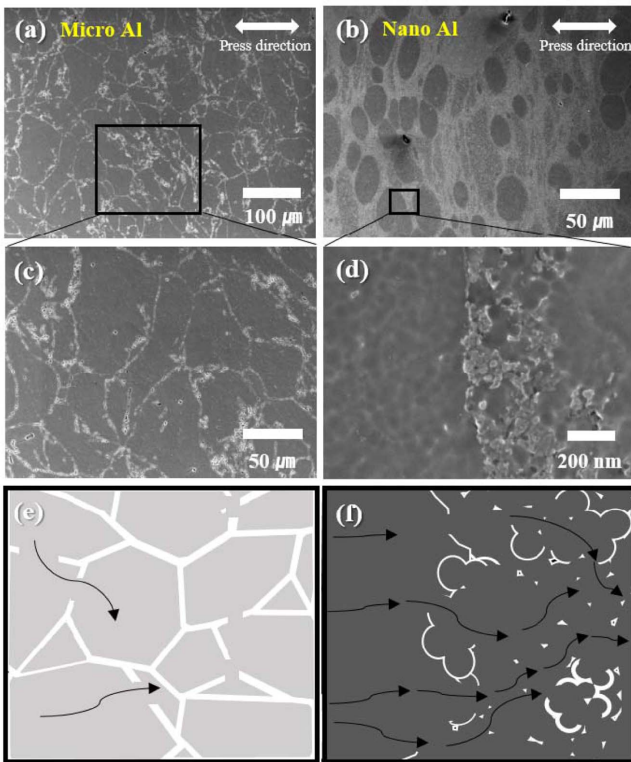
Further enhancement factors include the particle size and the degree of dispersion of the oxide. In the case of material manufactured by the powder metallurgy method, unlike the general casting method, the grain size of the alumina layer becomes larger due to the larger specific surface area of the powder Alumina is a typical ceramic material that is very brittle, and its hardness may be increased. Aluminum oxide is present in the bulk produced in this study. Alumina has a very high hardness value of 1400 to 1800 HV, and even if only a small amount is added to a material, the hardness of the material is considerably increased [17]. During the compaction process, the oxide layer existing on the powder surface is broken and dispersed in the form of nano particles. In case of nano Al, a very fine alumina layer may be dispersed in the bulk. Rahimian *et al.* studied the effect of the particle size of alumina dispersed in an Al matrix on the mechanical properties of the composite [18]. Hardness tends to increase with a decrease in alumina particle size within 10  $\mu m$ , indicating that the mechanical properties of nano particle Al can be further improved. In addition, alumina oxide can be strengthened by the effect of inhibiting grain growth through the pinning effect at the grain boundaries [19].

However, because these oxides have very low electrical conductivity, the Al-Al<sub>2</sub>O<sub>3</sub> composite is well known for its excellent mechanical properties; however, its electrical properties are not reported. On the other hand, the nano Al in this study showed electric conductivity when the amount of alumina produced was controlled. It is generally understood that the larger the grain size, the lower the electrical conductivity, because the electrical conduction is relatively difficult at disordered grain boundaries. However, the electrical conductivities of micro Al and nano Al were approximately 0 S/m, and  $2.170 \times 10^4$  S/m, as shown in Table 1. To analyze the reason for this phenomenon, we analyzed the oxygen content of each powder and bulk. As a result, the 2.66 wt.% of micro Al powder and the 2.79 wt.% of bulk were increased by 0.13 wt.% (Table 1).

On the other hand, in the case of nano Al powder, the oxygen content was 0 wt.% because the process was processed in an environment of less than 1 ppm oxygen content with non-oxidized Al powder, whereas the bulk was oxidized to 1.48 wt.% due to oxidization after fabrication. However, when com-

**Table 1.** Experimental mechanical and other properties of nano and micro size Al compacted under 1.2 GPa at room temperature

Material	Particle size	Oxygen content		Density		Vickers hardness (HV)	Electrical conductivity (S/m)
		Powder (wt. %)	Bulk (wt. %)	Experimental (g/cm <sup>3</sup> )	Relative (%)		
Al	Nano	0	1.48	2.64 ± 0.20	97.83 ± 7.49	79.60 ± 16.47	2.470 × 10 <sup>4</sup>
	Micro	2.67	2.79	2.68 ± 0.03	99.52 ± 1.11	44.11 ± 1.646	0

**Fig. 9.** SEM images of (a) micro Al, (b) nano Al, (c) high magnification of (a), and (d) high magnification of (b); illustration of microstructure of (e) SEM image of micro Al (c), and (f) nano Al (d)

paring the bulk itself, the oxygen content of nano Al was much lower than that of micro Al. In general, metal particles react with oxygen through the surface to form oxides. The thickness of the oxide layer produced at this time was almost constant regardless of the grain size at temperatures below 700 K [20]. Therefore, nano Al powder with a specific surface area  $1.5 \times 10^3$  times larger than micro Al powder is considered to be partially oxidized. This phenomenon results from the oxidation that occurs after it is made into bulk, because the production and processing have proceeded in an environment with very low oxygen content. Thus, oxidation occurs at the cracks and surfaces of the open pores after the particles have already formed a neck and are connected. For this reason, when electric conductivity is measured, it is considered that the electric conductivity of the nano Al will be rather high. In the case of micro Al, compaction occurs in the state when the oxide layer is forming in all the powders, so the oxide layer may break due

to the high pressure. However, the oxide layer is entirely maintained between the layers.

Fig. 9 shows the electrical conduction process in micro Al and nano Al. In the case of Micro Al, compaction occurs in the state when the oxide layer is forming in all the powders, so the oxide layer may break due to the high pressure. However, the oxide layer is entirely maintained between the layers. As a result, it is evident that a high-strength lightweight nano-crystalline Al material capable of conducting electricity can be manufactured by a high-pressure compaction method even though it has a fine grain size.

#### 4. CONCLUSIONS

In this study, high density bulk was produced by uniaxial direction compression of pure aluminum at room temperature. The microstructure and mechanical properties of the bulk as a function of the powder particle size were investigated by molding micro Al and nano Al at the same pressure.

Characterization of microstructures after compaction was compared according to compaction mechanism and particle size. The mechanical properties of each Al bulk were determined by the Vickers hardness test and nanoindentation. First, the mechanical properties can be improved by powder metallurgy. And the mechanical properties is affected on particle size of powder. In the case of nano Al, the Vickers hardness value was five to ten times the hardness of pure Al, which is generally expected. This strengthening phenomenon was analyzed by grain size refinement, oxide particle size refinement, and dispersion degree.

Also, by measuring the electrical conductivity, it was proved that electric conduction is possible even with a small grain size. As a result, it can be concluded that a high-strength lightweight material having electrical conductivity can be manufactured through high-pressure molding at room temperature. The material in this study shows the possibility of ultra-light and high-strength material. In conclusion, this research provides a basic study about the effect of the particle size of Al powder. A more quantitative analysis will be conducted in the future.

#### REFERENCES

1. Zhao, N., Nash, P., and Yang, X., "The Effect of Mechanical Alloying on Sic Distribution and the Properties of 6061 Aluminum Composite", *Journal of Material Processing and Technology*,

- Vol. 170, 2005, pp. 586-592.
2. Kwon, H., Park, D.H., Silvain, J.F., and Kawasaki, A., "Investigation of Carbon Nanotube Reinforced Aluminum Matrix Composite Materials", *Composites Science and Technology*, Vol. 70, 2010, pp. 546-550.
  3. Park, K., Park, J., and Kwon, H., "Fabrication and Characterization of Al-SUS316L Composite Materials Manufactured by the Spark Plasma Sintering Process", *Materials Science and Engineering A*, vol. 691, 2017, pp. 8-15.
  4. Meyers, M.A., Mishra, A., and Benson, D.J., "Mechanical Properties of Nanocrystalline Materials", *Progress in Materials Science*, Vol. 51, No. 4, 2006, pp. 427-556.
  5. Hirayama, Y., Suzuki, K., Yamaguchi, W., and Takagi, K., "Cold Welding Behavior of Fine Bare Aluminum Powders Prepared by New Low Oxygen Induction Thermal Plasma System", *Journal of Alloys and Compounds*, Vol. 768, 2018, pp. 608-612.
  6. Ye, J., Ajdelsztajn, L., and Schoenung, J.M., "Bulk Nanocrystalline Aluminum 5083 Alloy Fabricated by a Novel Technique: Cryomilling and Spark Plasma Sintering", *Metallurgical and Materials Transactions A*, Vol. 37, 2006, pp. 2569-2579.
  7. Fang, Z.Z., Wang, Z., Ryu, T., Hwang, K.S., and Sohn, H.Y., "Synthesis, Sintering and Mechanical Properties of Nanocrystalline Cemented Tungsten Carbide- A Review", *International Journal of Refractory Metals & Hard Materials*, Vol. 27, 2008, pp. 288-299.
  8. Grasso, S., Yoshida, H., Porwal, H., Sakka, Y., and Reece, M., "Highly Transparent  $\alpha$ -alumina Obtained by Low Cost High Pressure SPS", *Ceramic International*, Vol. 39, 2013, pp. 3243-3248.
  9. Hatch, J.E., *Aluminum: Properties and Physical Metallurgy*. American Society for Metals, Ohio, 1984, p 424.
  10. Srivatsan, T.S., Woods, R., Petratoli, M., and Sudarshan, T.S., "An Investigation of the Influence of Powder Particle Size on Microstructure and Hardness of Bulk Samples of Tungsten Carbide", *Powder Technology*, Vol. 122, 2002, pp. 54-60.
  11. Smith, William F; Hashemi, Javad, *Foundations of Materials Science and Engineering*, (4th ed.), McGraw-Hill, 2006.
  12. Furukawa, M., Iwahashi, Y., Horita, W., Nemoto, M., Tsenev, N.K., Valiev, R.Z., and Langdon, T.G., "Structural Evolution and the Hall-Petch Relationship in an Al Mg Li Zr Alloy with Ultra-fine Grain Size", *Acta Materialia*, vol. 45, 1997, pp. 4751-4757.
  13. Sato, Y.S., Park, S.H.C., and Kohawa, H., "Microstructural Factors Governing Hardness in Friction-stir Welds of Solid-solution-hardened Al Alloys", *Metallurgical and Materials Transactions A*, Vol. 32, 2001, pp. 3033-3042.
  14. Liu, Z.C., Lin, J.P., Li, S.J., and Chen, G.L., "Effects of Nb and Al on the Microstructures and Mechanical Properties of High Nb Containing TiAl Base Alloys", *Intermetallics*, Vol. 10, 2002, pp. 653-659.
  15. Jang, J.S.C., and Koch, C.C., "The Hall-Petch Relationship in Nanocrystalline Iron Produced by Ball Milling", *Scripta Metallurgica et Materialia*, Vol. 24, 1990, pp. 1599-1604.
  16. Farhat, Z.N., Ding, Y., Northwood, D.O., and Alpas, A.T., "Effect of Grain Size on Friction and Wear of Nanocrystalline Aluminum", *Materials Science and Engineering A*, Vol. 206, 1996, pp. 302-313.
  17. From Wikipedia, the Free Encyclopedia, [https://en.wikipedia.org/wiki/Aluminium\\_oxide](https://en.wikipedia.org/wiki/Aluminium_oxide), 5 January 2019.
  18. Rahimian, M., Parvin, N., and Ehsani, M., "Investigation of Particle Size and Amount of Alumina on Microstructure and Mechanical Properties of Al Matrix Composite Made by Powder Metallurgy", *Materials Science and Engineering A*, Vol. 527, 2010, pp. 1031-1038.
  19. Kwon, H., Park, D.H., Park, Y., Silvain, J.F., Kawasaki, A., and Park, Y., "Spark Plasma Sintering Behavior of Pure Aluminum Depending on Various Sintering Temperatures", *Metals and Materials International*, Vol. 16, 2010, pp. 71-75.
  20. Voroshtov, A.B., Lerner, M., Redkevich, N., Nie, H., Abraham, A., and Schoenitz, M., "Oxidation of Nano-sized Aluminum Powders", *Thermochimica Acta*, Vol. 636, 2016, pp. 48-56.